

# Low temperature synthesis and magneto-electrical studies in $\text{Nd}_{1-x}\text{Pb}_x\text{MnO}_3$ system

R. K. DWIVEDI, M. RAGHAVENDRA RAJ, D. BAHADUR\*

*Department of Metallurgical Engineering and Materials Science, Indian Institute of Technology Bombay, Mumbai 400076 India*  
E-mail: dhiren@met.iitb.ac.in

Published online: 08 July 2005

The system  $\text{Nd}_{1-x}\text{Pb}_x\text{MnO}_3$  with  $x \leq 0.50$  has been synthesized by citrate-gel route. All these samples have shown single phase structure with cubic symmetry. Magnetic and electrical behavior has been studied in the temperature range 4–300 K. The temperature dependent resistivity data shows that metal-semiconductor transitions occurs at temperature  $T_P \sim 166, 174$  and  $182$  K for  $x = 0.30, 0.40$  and  $0.50$  respectively. Under the field of  $1 T$ , this transition shifts to higher temperature. These samples have shown maximum MR upto 40% under the field of  $1 T$  at temperature lower than  $T_P$ . These results are supported by magnetic measurements over the observed temperature range. Resistivity data above  $T_P$  has been found to fit well with  $T^n$  where  $n = -1/4$  for  $x = 0.30$  and  $n = -1/2$  for  $x = 0.50$  which is attributed to the variable range hopping of small polarons.  
© 2005 Springer Science + Business Media, Inc.

## 1. Introduction

The colossal magneto resistance (CMR) properties of hole doped manganites of the type  $\text{Ln}_{1-x}\text{A}_x\text{MnO}_3$ , where  $\text{Ln} = \text{La}, \text{Nd}$ , etc. and  $\text{A} = \text{Ba}, \text{Ca}, \text{Pb}, \text{Sr}$ , have drawn the attention for last one decade [1–5]. The substitution of divalent alkaline earth ions on A sites leads to mixed valency of Mn ( $\text{Mn}^{3+}/\text{Mn}^{4+}$ ) ions which occupy B-sites of these manganites. Depending on the substitution and average size of A-site cations, these compounds exhibit rich magnetic and electrical properties such as anti-ferromagnetic insulator (AFI), ferromagnetic insulator (FMI), ferromagnetic metal (FMM), and paramagnetic insulator [6]. For compositions within the range  $0.2 < x < 0.5$ , there have been metal-insulator transition (MI) associated to ferromagnetic-paramagnetic (FM-PM) transition. PM-FM transition is accompanied by a sharp drop in resistivity ( $\rho_T$ ). Recently, interest in these materials has been renewed by the realization that the magneto-resistance associated with the correlation between magnetization  $M$  and resistivity  $\rho$  can be very large. The FM and the mechanism of CMR in mixed valence manganite had been interpreted on the double exchange interaction model where motion of an  $e_g$  electron occurs between  $\text{Mn}^{3+}$  to  $\text{Mn}^{4+}$  ions [7–9] and this has been found insufficient to explain all features of the results [10]. Recently, other factors, particularly the strong electron-phonon coupling due to local Jahn-Teller (JT) distortion of  $\text{Mn}^{3+}$  [10] ions as well as lattice strain and deformations that affect the  $\text{Mn}^{3+}-\text{O}-\text{Mn}^{4+}$  bond angle and

length [11, 12] have been proposed to play a key role in the exotic properties of these compounds.

For the possible technological applications, good magneto-transport properties, at or close to ambient temperature, are required. In this context, Pb doped perovskites, exhibit critical temperature close to 300 K [13, 14] and offer the possibility of realizing a technologically useful magneto-resistive effect near the room temperature. Extensive research has been carried out in lead doped manganites in its single crystalline forms [13, 15, 16] and to some extent in polycrystalline form [17–19]. However, the research in polycrystalline manganites have been restricted due to evaporation of lead, which leads to non stoichiometry in the compounds, while the compounds are synthesized at temperatures more than  $900^\circ\text{C}$ . Maintaining a PbO atmosphere in the furnace has become a conventional procedure to compensate PbO loss which obviously can not impart perfect homogeneity and uniform microstructure to the final products. In order to maintain better homogeneity and stoichiometry, it is highly desirable to bring down reaction temperature below the melting point of PbO i.e.  $880^\circ\text{C}$  [20]. In view of this, it has been essential to use such a route which can produce fine powders and hence can be used to synthesize these compounds at such a temperatures at which, lead loss can be avoided and stoichiometry can be assured.

We have investigated  $\text{Nd}_{1-x}\text{Pb}_x\text{MnO}_3$  manganite system. In this process, an effort has been made to synthesize samples at the lower temperatures by using

\*Author to whom all correspondence should be addressed.

citrate-gel route by optimizing the ratio of the metal ions to citric acid (M/C) by weight for a particular composition  $x = 0.20$ . The process of crystallization has been studied using X-ray diffraction studies. In this communication, we report the optimization of the ratio of metal ions to citric acid on the formation of single phase solid solution at lowest possible temperatures, effect of variation of  $x$  on magnetic and electrical properties in the system  $\text{Nd}_{1-x}\text{Pb}_x\text{MnO}_3$ . The composition with  $x = 0.30$ , one of the compositions in the present system has been studied earlier by Gutierrez *et al.* [19], Blanco *et al.* [21] and Young *et al.* [22]. We have restricted these studies within the composition range  $0.20 \leq x \leq 0.50$ , because most of the manganites exhibit useful electrical and magnetic properties in this range only. To the best of my knowledge, the system has been synthesized first time at such a low temperature.

## 2. Experimental

Compositions with  $x = 0.20, 0.30, 0.40$  and  $0.50$  in the system  $\text{Nd}_{1-x}\text{Pb}_x\text{MnO}_3$  were synthesized by citrate-gel process. For this, appropriate amounts of  $\text{PbCO}_3$  and  $\text{Nd}_2\text{O}_3$  (each oxides of purity more than 99.9%) were dissolved into  $\text{HNO}_3$  to form nitrates of these metal ions separately for each composition followed by mixing and warming on to a hot plate. After warming the mixture of above nitrate solutions, manganese acetate was added into this solution with continuous stirring followed by adding appropriate amount of citric acid.

In order to get appropriate gel formation, the amount of citric acid, added to nitrate solution, was optimized for a particular composition with  $x = 0.20$ . For this, metal ions to citric acid (M/C) ratio of 1:1, 1:2, 1:3 and 1:4 by weight have been tried. When the solution turns into a transparent clear liquid, appropriate amount of ethylene glycol was added into this solution with continuous stirring. The pH of the solution was controlled by adding ammonia solution to it. The clear transparent solution, on heating, becomes brown and finally turns into viscous gel. This was further replaced in an oven at  $150^\circ\text{C}$  for 24 h. The gel transformed into fluffy dried mass, which was ground and heat treated at  $550, 600, 650$  and  $700^\circ\text{C}$  successively for 12 h. XRD patterns of these samples were recorded using X-Ray Diffractometer (Philips PW 1729) with  $\text{Cu-K}\alpha$  radiation. Following the most appropriate M/C ratio  $\sim 1:3$  (found to produce a better crystallized phase at  $550^\circ\text{C}$ ), all the other compositions with  $x = 0.30, 0.40$  and  $0.50$  were prepared and followed by calcination at  $700^\circ\text{C}$  for 12 h. These powders were compacted, sintered at  $850^\circ\text{C}$  and used for resistivity measurement. The temperature dependence of resistivity ( $\rho_T$ ) and MR of these pellets were measured by standard four probe technique in the temperature range  $80\text{--}300\text{ K}$  as described elsewhere [23]. A VSM was used for measurement of magnetization  $M$  down to  $4.2\text{ K}$  at  $0.5\text{ T}$ .

## 3. Results and discussion

X-ray diffraction patterns of the composition with  $x = 0.20$  in the system  $\text{Nd}_{1-x}\text{Pb}_x\text{MnO}_3$  for different metal

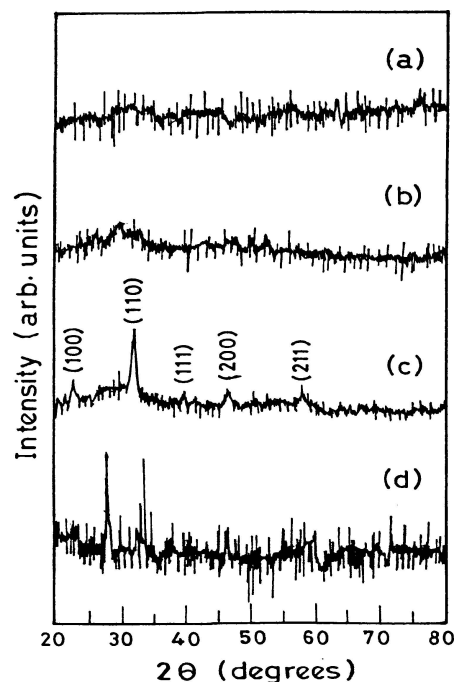


Figure 1 X-ray diffraction patterns of composition  $\text{Nd}_{0.80}\text{Pb}_{0.20}\text{MnO}_3$  with metal ions to citric acid ratio (a) 1:1, (b) 1:2, (c) 1:3 and (d) 1:4 heat treated at  $550^\circ\text{C}$  for 12 h.

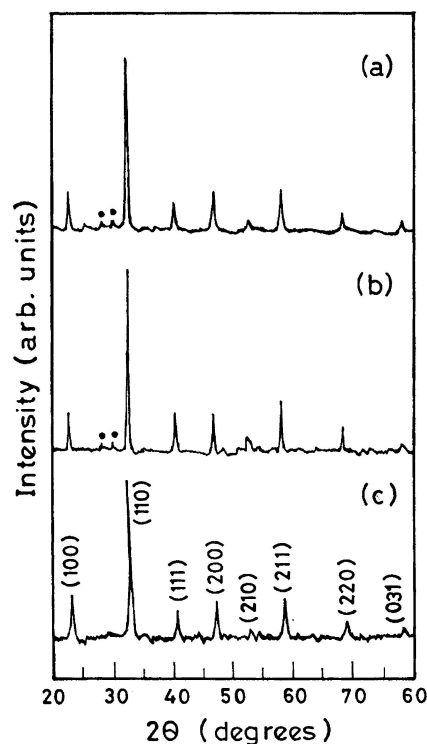


Figure 2 X-ray diffraction patterns of composition  $\text{Nd}_{0.80}\text{Pb}_{0.20}\text{MnO}_3$ , with M/C ratio = 1:3, calcined at (a)  $600^\circ\text{C}$  (b)  $650^\circ\text{C}$  and (c)  $700^\circ\text{C}$ . (• represents unwanted phase).

ions to citric acid (M/C) ratio are shown in Fig. 1. These samples were heated at  $550^\circ\text{C}$  for 12 h. A careful examination of the XRD patterns reveals the existence of the growth of manganite phase with decreasing the metal ions to citric acid ratio (M/C) from 1:1 to 1:4 i.e. with increasing proportion of citric acid (Figs 1a–d). It is observed that the best crystallization of manganite phase occurs for sample with metal ions to citric acid ratio of 1:3 (Fig. 1c). The same composition ( $x = 0.20$ ), however, when heated at  $600$  and  $650^\circ\text{C}$

TABLE I Structure, lattice parameter, resistivity peak temperature without field ' $T_p$ ', resistivity at room temperature ' $\rho_0$ ' and average A-site ionic radii ' $r_{<A>}$ ' for the compositions  $x$  in the system  $\text{Nd}_{1-x}\text{Pb}_x\text{MnO}_3$

$x$	Structure	Lattice parameters $a$ (Å)	Tolerance factor ' $t$ '	$T_p$ (K)	$\rho_0$ (ohm cm)	$r_{<A>}$
0.20	cubic	3.841	0.9491	—	34.18	1.31
0.30	cubic	3.846	0.9623	166	28.63	1.34
0.40	cubic	3.851	0.9756	172	8.52	1.36
0.50	cubic	3.859	0.9891	182	1.76	1.38

for 12 h shows the presence of unreacted phase (Figs 2a and b). The unreacted phase disappears upon heating (calcining) at  $700^\circ\text{C}$  for 12 h (Fig. 2c). Complete single phase compound, thus obtained, has been indexed on the basis of cubic structure. Similarly, the other compositions with  $x = 0.30, 0.40$  and  $0.50$ , when prepared with M/C ratio  $\sim 1:3$  and calcined at  $700^\circ\text{C}$  for 12 h, have shown single phase formation with cubic symmetry. Lattice parameter, determined using least square fitting of the diffraction data, for these compositions are given in Table I which is consistent with the reported cell constant for a single crystal of a particular composition  $\text{Nd}_{0.50}\text{Pb}_{0.50}\text{MnO}_3$  [16].

The approximate value of particle size has been determined using Scherrer's formula from the broadening of the line which corresponds to the diffraction line at  $2\theta \approx 32.65^\circ$  (or  $I/I_0 = 100$ ). The particle size is estimated around 24 nm. Increasing the temperature of the heating schedule results in the sharpening of the diffraction lines, reflecting growth in the crystallinity of these samples (Fig. 2c).

Figs 3a–d show variation of resistivity ( $\rho_T$ ) with temperature under an applied field of 1 T and without field for compositions  $x = 0.20, 0.30, 0.40$  and  $0.50$ . It has been observed that composition with  $x = 0.20$  shows insulating behavior with and without field throughout the observed temperature range. Whereas a zero field resistivity peak appears at temperatures ( $T_p$ ) 166, 174 and 182 K respectively for  $x = 0.30, 0.40$  and  $0.50$ . The applied field of 1 T considerably reduces the peak resistivity and shifts the peak temperature ( $T_{PF}$ ) upward, which is found to be consistent with previous observations on related materials [16, 17, 24]. Further, on careful observation of the results, the changeover from negative MR to positive MR (see Fig. 3) for  $x = 0.30$  and  $x = 0.40$  occurs at  $T > T_{PF}$  while for  $x = 0.50$ , it occurs at exactly  $T_{PF}$ . Similar changeover is reported by Khajeni *et al.* [17] and Shapira *et al.* [25] which occurs due low magnetic field applied on the sample. MR% has been determined using the formula:

$$\%MR = -\left[\frac{\rho(T) - \rho(0)}{\rho(0)}\right] * 100$$

where  $\rho(0)$  and  $\rho(T)$  are the resistivity under zero field and an applied field of 1 T respectively [1].

The maximum MR values, obtained around metal-insulator transition, are in between 30 to 40%. It increases with increasing  $x$ . Further it has been noticed that the value of peak resistivity decreases with increasing concentration of Pb.

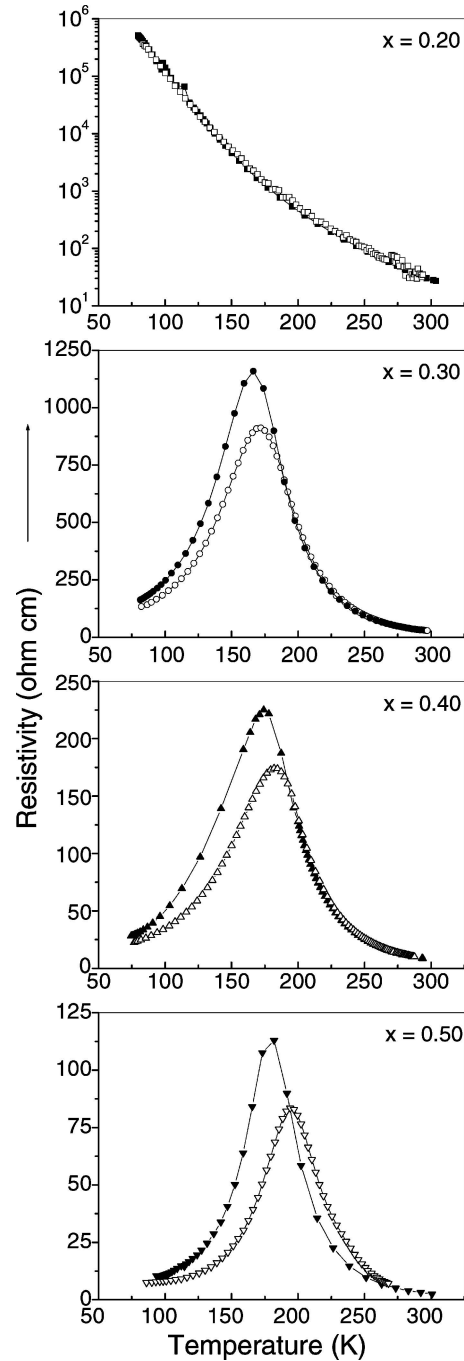


Figure 3 Temperature dependent resistivity  $\rho(T)$  plots with magnetic field  $\sim 1$  T and with zero field for compositions with  $x = 0.20, 0.30, 0.40$  and  $0.50$  in the system  $\text{Nd}_{1-x}\text{Pb}_x\text{MnO}_3$ . Symbol 'o' represents data with field  $\sim 1$  T and '•' with zero field (ZFC).

Magnetic studies for the typical compositions with  $x = 0.30, 0.40$  and  $0.50$ , which show metal to semiconductor transition, have been made. Magnetization vs temperature plots for these compositions are shown in Fig. 4. Two magnetic transitions are obtained, the first one at 200 K corresponds to the PM to FM transition, though the magnetization value is lower for  $x = 0.50$ . The second transition around 50 K is accompanied by reduction in magnetization. Such transitions have been reported in many systems and has been attributed the transformation to the AFM charge ordered state [26]. In fact, the co-existence of ferromagnetism and incommensurate charge ordering has been invoked in similar systems to explain the two magnetic transitions in this

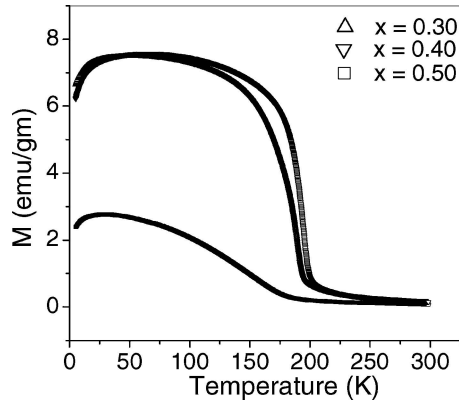


Figure 4 Magnetization vs. Temperature plots for  $x = 0.30, 0.40$  and  $0.50$  in the system  $\text{Nd}_{1-x}\text{Pb}_x\text{MnO}_3$ .

system. It has been observed that magnetization, for  $x = 0.30$  and  $0.40$ , rises sharply around  $195\text{ K}$  while samples are cooled in presence of an applied field of  $5\text{ kOe}$ . This reveals that paramagnetic to ferromagnetic transition occurs around this temperature. The composition with  $x = 0.50$  shows slightly different behavior and for this sample magnetization rises slowly below  $185\text{ K}$ . This sample has shown lower magnetization as compared to other samples. All these samples show decrease in magnetization at temperatures  $< 50\text{ K}$ . This is a typical characteristic of a transition to anti-ferromagnetic state.

The temperature dependent resistivity  $\rho(T)$  data above peak temperature ( $T_P$ ) has been analyzed by plotting  $\log(\rho)$  as a function of  $T^n$  (Fig. 5) where

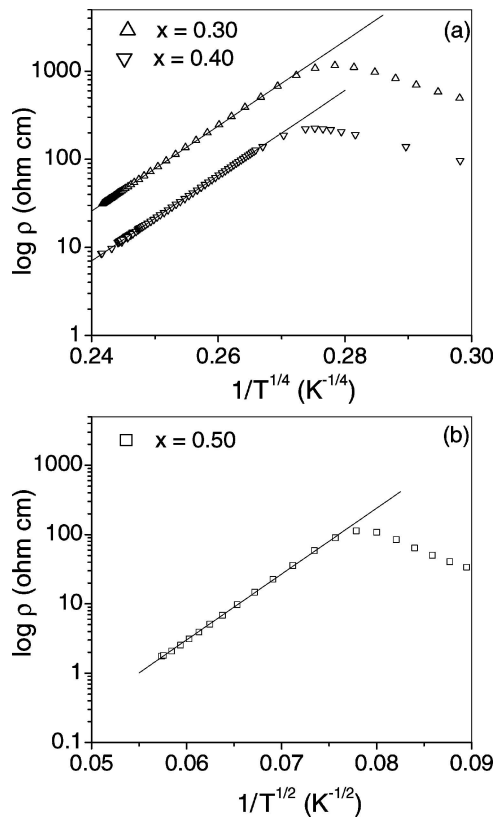


Figure 5 Plots of  $\log \rho$  with  $T^n$  for compositions  $x$  (a)  $0.30$  and  $0.40$ , where  $n = -1/4$ , and (b)  $0.50$ , where  $n = -1/2$  in the system  $\text{Nd}_{1-x}\text{Pb}_x\text{MnO}_3$ .

$n = -1, -1/2$  and  $-1/4$ .  $T^{-1}$  law, a characteristic of nearest neighbor hopping or activation to a mobility edge, could not be fitted to our data.  $T^{-1/2}$  law, which concerns variable range hopping (VRH) with a soft gap due to electron correlation, has been found to fit the data well for the compositions with  $x = 0.50$ . The data for  $x = 0.30$  can be fitted well according to the expression:

$$\ln(\rho/\rho_0) = (T_0/T)^{1/4}$$

which indicates variable range hopping of electrons in the band of localized states in the absence of electron-electron interactions [27, 28].

From magnetization data, it is clear that transitions from paramagnetic spin disordered state to ferromagnetic spin ordered state occurs above the temperature of the resistivity peak. Kuster *et al.* [16] have reported that Single crystal of composition  $\text{Nd}_{0.50}\text{Pb}_{0.50}\text{MnO}_3$  shows resistivity peak at  $184\text{ K}$ . However, there is a contradiction with the fitting of resistivity data above  $190\text{ K}$ .

For composition with  $x = 0.50$ , it is expected that ratio of  $\text{Mn}^{3+}$  and  $\text{Mn}^{4+}$  is  $1:1$  which may lead to orbital ordering through coulomb interaction. This coulomb interaction via electron correlation may create the ground for soft gap formation between localized electrons near the Fermi surfaces. This also supports the fitting of our resistivity data above transition temperature with  $T^{-1/2}$  law, which is valid for variable range hopping with soft gap conduction. In contradiction to this, Kusters *et al.* [16] have observed that resistivity decreases exponentially above  $T_P$ , indicating activated transport. This difference may occur due to absence of grain-boundaries in his samples.

The observed resistivity behavior above  $T_C$  is indicative of conduction by formation of magnetic polarons [1]. A magnetic polaron is a conducting electron, which polarizes magnetic moments of the surrounding ions, forming a small ferromagnetic region. Magnetic polarons could become polarized as a result of magnetic interaction as was originally suggested by Mott [27]. Conduction by localized magnetic polarons then proceeds via a variable range hopping process.

Below the transition temperature  $T_C$ , the formation of magnetic polarons becomes impossible due to the ferromagnetic ordering of the materials. The collapse of the hopping behavior of the magnetic polarons results in the drop of the resistivity. The application of an external magnetic field increases the ferromagnetic ordering and suppresses the formation of magnetic polarons leading to the MR near  $T_C$  i.e. close to  $T_P$ . Further it shifts the broad resistivity peak to higher temperature i.e.  $T_{PF}$ . The increase in the transition temperature can also be interpreted as a consequence of increased electronic hopping amplitude as a function of magnetic field [7–9].

In such perovskite systems, a discussion on  $r_{<A>}$  invokes the tolerance factor ‘ $t$ ’ a geometrical quantity defined as  $t = d_{A-O}/\sqrt{2}(d_{\text{Mn-O}})$ . This factor is a simple characterization of a size mismatch that occurs when A-site ions are too small to fill the space in the three dimensional network of  $\text{MnO}_6$ . For a perfect size match ( $t = 1$ ), the Mn–O–Mn bond angle  $\theta$  would be  $180^\circ$ .

For  $t < 1$ , rather than a simple contraction of a bond distances, the octohedra tilts and rotates to reduce the excess space around the A-sites resulting in  $\theta < 180^\circ$ . It has to be noticed from Table I that the tolerance factor increases with  $x$  from 't' = 0.9491 for  $x = 0.20$  to 0.9891 for  $x = 0.50$ . This shows that Mn—O—Mn bond angle  $\theta < 180^\circ$  for  $x = 0.20$  and becomes closer to  $\theta = 180^\circ$  for  $x = 0.50$ . Further, when Mn-O-Mn bond angle deviates from  $\theta = 180^\circ$ , the mobility of the electron decreases and hence lead to increase in resistivity. This seems to be the reason why the resistivity for  $x = 0.30$  is higher. The reason for anomalous rise in resistivity by several order of magnitude for  $x = 0.20$  than other compositions, may be attributed to the absence of FM state in this sample which reveals that  $Mn^{4+}$  concentration is not enough to induce ferromagnetism. No magnetoresistance has been observed for this composition over the observed temperature range.

In summary, compositions within the range  $x \leq 0.50$  in the  $Nd_{1-x}Pb_xMnO_3$  system have been synthesized. All these compositions have shown single phase formation with cubic symmetry. The electrical and magnetic data has been studied for compositions  $0.20 \leq x \leq 0.50$ . It has been found that metal-semiconductor transition has been induced for  $x \geq 0.30$ . This transition shifts to higher temperatures with increasing  $x$ . This also corresponds to magnetic transition from paramagnetic to ferromagnetic state. There seems to be another magnetic transition below 50 K, which is typical of anti-ferromagnetic charge ordered transition. For these compositions, maximum MR has been found to be 30–40% near the transition temperatures. Conduction appears to be dominated by the formation of magnetic polarons at temperature above the transition temperatures.

### Acknowledgements

We are thankful to Department of Science and Technology, Government of India for financial support to these investigations.

### References

1. R. VON HELMOLT, J. WECKERG, B. HOLZAFEL, L. SCHULTZ and K. SAMWER, *Phys. Rev. Lett.* **71** (1993) 2331.
2. K. CHAHARA, T. OHNO, M. KASAI and Y. KOZONO, *App. Phys. Lett.* **63** (1993) 1990.
3. A. URUSHIBARA, Y. MORITOMO, T. ARIMA, A. ASAMITSU, G. KIDO and Y. TAKURA, *Phys. Rev. B* **51** (1995) 14103.
4. R. MAHENDIRAN, S. K. TIWARI, A. K. RAYCHAUDHURI, T. V. RAMKRISHNAN, R. MAHESH, N. RANGAVITTAL and C. N. R. RAO, *ibid.* **53** (1996) 3348.
5. H. KUWAHARA, Y. TOMIOKA, A. ASAMITSU, Y. MORITOMO and Y. TOKURA, *Science* **270** (1995) 961.
6. G. H. JONKER and J. H. VAN SANTEN, *Physica* **16** (1950) 337.
7. S. K. VIJAYA, P. V. VANITHA, RAM SESHADRI, A. K. CHETAM and C. N. RAO, *Chem. Mat.* **13** (2001) 787.

8. C. ZENER, *Phys. Rev.* **82** (1951) 403.
9. P. W. ANDERSON and H. HASEGAWA, *ibid.* **100** (1955) 675.
10. P. G. DE GENNES, *Phys. Rev.* **118** (1960) 141.
11. A. J. MILLIS, P. B. LITTLEWOOD and B. SHRAIMAN, *Phys. Rev. Lett.* **74** (1995) 5144; A. J. MILLIS, B. SHRAIMAN and I. MUELER, *ibid.* **77** (1996) 175.
12. H. Y. HWANG, H. W. CHEONG, P. G. RADIELLI, M. MAREZIO and B. BATLOG, *ibid.* **75** (1995) 914.
13. L. M. RODRIGUEZ-MARTINEZ and J. PAUL ATTFIELD, *Phys. Rev. B* **R15** (1996) 622.
14. C. W. SEARL and S. T. WANG, *Can. J. Phys.* **47** (1969) 2703; C. W. SEARL and S. T. WANG, *Can. J. Phys.* **48** (1970) 2023.
15. A. V. POWEL, C. HERWING, D. C. COLGAN and A. G. WHITTAKER, *J. Mat. Chem.* **8** (1998) 119.
16. R. M. KUSTERS, J. SINGELETON, D. A. KEEN, R. MCGREEVY and W. HAYES, *Physica (Amsterdam)* **155B** (1989) 362.
17. K. KHAZENI, Y. X. JIA, LU LI, H. CRESPI VINCENT, L. COHEN MARVIN and A. ZETT, *Phys. Rev. Lett.* **76** (1996) 295.
18. R. MAHINDRAN, R. MAHESH, A. K. RAYCHAUDHARI and C. N. R. RAO, *J. Phys. D: App. Phys.* **28** (1995) 1743.
19. J. GUITIERREZ, A. PENA, J. M. BARANDIARAN, J. L. PIZARRO, T. HERNANDEZ, L. LEZAMA, M. INSAUSTI and T. ROZO, *Phys. Rev. B* **61** (2000) 9028; J. GUITIERREZ, J. M. BARANDIARAN, M. INSAUSTI, L. LEZAMA, A. PENA, J. J. BLANCO and T. ROZO, *J. App. Phys.* **83** (1998) 7171.
20. SRINIVASA Y. RAO and C. S. SUNANDANA, *Mat. Sci. Lett.* **11** (1992) 595.
21. J. J. BLANCO, L. LEZAMA, M. INSAUSTI, J. GUITIERREZ, J. M. BARANDIARAN and T. ROZO, *Chem. Mater.* **11**(12) (1999) 3464.
22. S. L. YOUNG, Y. C. CHEN, LANCE HORNG, T. C. WU, C. C. CHANG, H. Z. CHEN and J. B. SHI, *J. Magnetism and Magnetic Materials* **239** (2002) 11.
23. D. DAS, P. CHOWDHARY, R. N. DAS, C. M. SRIVASTAV, A. K. NIGAM and D. BAHADUR, *ibid.* **238** (2002) 178.
24. Y. X. JIA, L. LU, K. KHAJENI, D. YEN, C. S. LEE and A. ZETTL, *Solid State Commun.* **94** (1995) 917; Y. X. JIA, L. LU, K. KHAJENI, H. VINCENT CRESPI, M. L. COHEN A. P. SCHIFFER, A. P. RAMIREZ, W. BAO and S. W. CHEONG, *Phys. Rev. Letter* **75** (1995) 3336.
25. Y. SHAPIRA, S. PHONER, N. F. OLIVEIRA JR. and T. B. REED, *Phys. Rev. B* **10** (1974) 4765. [Abstract, a few lines: A negative magnetoresistance was observed for most temperatures and was very large near  $T_{max}$ . However, in the limited temperature range interval well above  $T_{max}$ , a positive magneto resistance was observed at low field followed by a negative resistance at higher fields].
26. C. N. R. RAO and P. V. VANITHA, *Current Opinion in Solid State Science* **6** (2002) 97.
27. N. F. MOTT, "Metal-Insulator Transitions," 2nd ed. (Taylor and Francis, 1990); N. F. MOTT and E. A. Davies, "Electronic Processes in Non Crystalline Materials" (Clarendon, Oxford, 1979).
28. D. BAHADUR, M. YEWONDWOSSEN, Z. KOZIAL, M. FOLDEAKI and R. A. DUNLAP, *J. Phys.: Condensed Matter* **8** (1996) 5235.

Received 18 August 2003

and accepted 3 February 2005